

Delayed-measurement one-way quantum computing on cloud quantum computer

Zhi-Peng Yang(杨智鹏), Yu-Ran Zhang(张煜然), Fu-Li Li(李福利), and Heng Fan(范桁)

Citation: Chin. Phys. B, 2024, 33 (**9**): 090304. DOI: 10.1088/1674-1056/ad6253
Journal homepage: http://cpb.iphy.ac.cn; http://iopscience.iop.org/cpb

What follows is a list of articles you may be interested in

Detecting the quantum phase transition from the perspective of quantum information in the Aubry-André model

Geng-Biao Wei(韦庚彪), Liu Ye(叶柳), and Dong Wang(王栋)
Chin. Phys. B, 2024, 33 (**7**): 070301. DOI: 10.1088/1674-1056/ad2f1f

Quantum circuit-based proxy blind signatures: A novel approach and experimental evaluation on the IBM quantum cloud platform

Xiaoping Lou(娄小平), Huiru Zan(昝慧茹), and Xuejiao Xu(徐雪娇)
Chin. Phys. B, 2024, 33 (**5**): 050307. DOI: 10.1088/1674-1056/ad22d5

Quantum correlations and entanglement in coupled optomechanical resonators with photon hopping via Gaussian interferometric power analysis

Y. Lahlou, B. Maroufi, and M. Daoud
Chin. Phys. B, 2024, 33 (**5**): 050303. DOI: 10.1088/1674-1056/ad2a6e

Quantum synchronization with correlated baths

Lei Li(李磊), Chun-Hui Wang(王春辉), Hong-Hao Yin(尹洪浩), Ru-Quan Wang(王如泉), and Wu-Ming Liu(刘伍明)
Chin. Phys. B, 2024, 33 (**2**): 020306. DOI: 10.1088/1674-1056/ad0bef

A proposal for preparation of cluster states with linear optics

Le Ju(鞠乐), Ming Yang(杨名), and Peng Xue(薛鹏)
Chin. Phys. B, 2021, 30 (**3**): 030306. DOI: 10.1088/1674-1056/abd74b

---

SPECIAL TOPIC — Quantum computing and quantum sensing

Delayed-measurement one-way quantum computing on cloud quantum computer

Zhi-Peng Yang(杨智鹏)[1,2], Yu-Ran Zhang(张煜然)[3], Fu-Li Li(李福利)[2], and Heng Fan(范桁)[4,1,†]

[1] *Beijing Academy of Quantum Information Science, Beijing* 100193, *China*
[2] *Ministry of Education Key Laboratory for Nonequilibrium Synthesis and Modulation of Condensed Matter, Shaanxi Province Key Laboratory of Quantum Information and Quantum Optoelectronic Devices, School of Physics, Xi'an Jiaotong University, Xi'an, Shaanxi* 710049, *China*
[3] *School of Physics and Optoelectronics, South China University of Technology, Guangzhou* 510640, *China*
[4] *Institute of Physics, China Academy of Sciences, Beijing* 100190, *China*

(Received 30 May 2024; revised manuscript received 26 June 2024; accepted manuscript online 12 July 2024)

One-way quantum computation focuses on initially generating an entangled cluster state followed by a sequence of measurements with classical communication of their individual outcomes. Recently, a delayed-measurement approach has been applied to replace classical communication of individual measurement outcomes. In this work, by considering the delayed-measurement approach, we demonstrate a modified one-way CNOT gate using the on-cloud superconducting quantum computing platform: Quafu. The modified protocol for one-way quantum computing requires only three qubits rather than the four used in the standard protocol. Since this modified cluster state decreases the number of physical qubits required to implement one-way computation, both the scalability and complexity of the computing process are improved. Compared to previous work, this modified one-way CNOT gate is superior to the standard one in both fidelity and resource requirements. We have also numerically compared the behavior of standard and modified methods in large-scale one-way quantum computing. Our results suggest that in a noisy intermediate-scale quantum (NISQ) era, the modified method shows a significant advantage for one-way quantum computation.

Keywords: measurement-based quantum computing, quantum entanglement, quantum gates

PACS: 03.65.Ud, 03.67.–a, 03.67.Ac, 03.67.Lx **DOI:** 10.1088/1674-1056/ad6253

1. Introduction

Compared to the standard quantum computing proposals based on circuit models with unitary-logic gates acting on physical qubits,[1–5] one-way quantum computation allows universal quantum computation by applying a series of single-qubit measurements on a cluster state or a graph state[6–10] with classical communication of their individual outcomes. One-way quantum computing simplifies complex operations in the circuit model in the sense that the requirements of gate fidelity and single-qubit coherence can be reduced.[11]

The scale of one-way quantum computing is not restricted by the number of available physical qubits and logic gates; instead, it is restricted by the scale of cluster state that one can generate.[12] Currently, large-scale 2-dimensional cluster states have been demonstrated in photonic systems.[13–15] Note that although in general, the cluster state generation is independent of the circuit model, the current proposals of large-scale cluster state generation still rely on applying unitary-logic gates on physical qubits. Nevertheless, by cooling the qubits, a cluster state may be generated more efficiently than the circuit model.[7]

With the concept of a cluster state, one-way quantum computing[6] was initially applied to a one-way CNOT protocol. Later, a complete set of one-way logic gates was theoretically proposed in Ref. [8]. In addition, the experimental realizations of one-way logic gates were initially demonstrated in photonic systems.[16] Over the past 15 years, numerous experimental demonstrations of one-way logic gates have been implemented in different physical systems, e.g., optical cavities,[13,14,17–22] trapped ions,[23] and nuclear magnetic resonance (NMR) system[24] (see also the review[25]).

More recently, another proposal for a one-way CNOT gate was proposed in Ref. [26]. In the circuit models, the standard one-way CNOT gate requires four qubits, while the modified one only needs three qubits. In this sense, the complexity of building a one-way CNOT gate decreases because of the lower circuit depth. Note that the cluster state used in this proposal does not strictly obey the criteria of cluster states. Thus, we denote it as a modified cluster state.

Since one-way quantum computing is based on cluster state preparation, the scalability of the system is an essential factor in achieving practical one-way quantum computing. Superconducting qubits[4,27–31] are considered one of the promising systems for building one-way quantum computation.[32–41] However, until very recently, the experimental demonstration of one-way quantum computation in superconducting circuits was still lacking.[42–45]

In this work, we performed a modified one-way CNOT

†Corresponding author. E-mail: hfan@iphy.ac.cn

© 2024 Chinese Physical Society and IOP Publishing Ltd

gate on Quafu.[46] We initially constructed the modified cluster state, and showed that this modified one-way CNOT gate can be realized using the delayed-measurement method. Thus, we can decrease the impact of measurement error and overcome the limitations of a quantum operation controlled by a classical register. Using the Quafu quantum processor, we have also compared the modified one-way CNOT gate with its standard counterpart and verified the advantage of the modified protocol. To study the properties of the modified one-way CNOT gate, we have simulated a series of processes that, respectively, carry out the modified and standard one-way CNOT gates in the presence of different noises. The numerical results indicate that the modified one-way CNOT gate is more robust against thermal error and gate error than the standard one. Also, our simulation results imply the advantage of the delayed-measurement method in enhancing the robustness against qubit measurement errors.

This article is organized as follows. Sections 2 and 3 briefly introduce the protocols of the standard and modified one-way CNOT gates, respectively. Section 4 introduces the delayed-measurement protocol for realizing a modified one-way CNOT gate and a standard one-way CNOT gate on a Quafu superconducting quantum chip, and presents the results. Section 5 numerically analyzes the advantage of the modified one-way CNOT gate over the standard one.

2. Standard protocol of one-way CNOT gate

In this paper, we label the qubits with different symbols. We denote the qubit that carries the input of the target state by $Q_{\rm I}$, and the qubit that carries the output of the target state is labeled as $Q_{\rm O}$. The qubit carries the control state is denoted by $Q_{\rm C}$. These qubits are called "functional qubits". In addition, we use $Q_{\rm A}$ to denote an ancilla qubit. When referring to physical qubits, including a subset of physical qubits on a quantum chip, we denote the qubits by Q_i, where the subscript i corresponds to the number of the physical qubit according to the Quafu website.

In order to realize a standard one-way CNOT gate, we first prepare the four-qubit cluster state by applying a series of conventional CZ gates, $U_{\rm CZ} = I \otimes |0\rangle\langle 0| + Z \otimes |1\rangle\langle 1|$, on the superposed state $|+\rangle = (|0\rangle + |1\rangle)/\sqrt{2}$ of $Q_{\rm A}$ and $Q_{\rm O}$ (as shown in Fig. 1). Here, Z represents a Pauli-Z operation. This state is defined in the computational basis $|0\rangle$ and $|1\rangle$. After entangling all the qubits, we measure $Q_{\rm I}$ and $Q_{\rm A}$ on the σ_x basis, and obtain the results s_1 and s_2, respectively. Here, s_1, $s_2 = 0$ (1) corresponds to the eigenstate $|+\rangle$ ($|-\rangle$) of the σ_x operator,

$$\sigma_x = \begin{bmatrix} 0 & 1 \\ 1 & 0 \end{bmatrix}, \tag{1}$$

for the physical qubits Q_1 and Q_2, respectively. Finally, we apply a series of Pauli gates on qubits $Q_{\rm O}$ and $Q_{\rm C}$ which are decided by s_1 and s_2:

$$U_{\rm F} = Z_{\rm O}^{s_1+1} X_{\rm O}^{s_2} \otimes Z_{\rm C}^{s_1}, \tag{2}$$

where $Z_i = \sigma_{z,i}$ and $X_i = \sigma_{x,i}$ denote the Pauli-Z and Pauli-X operations acting on the functional qubit Q_i. In this way, the state on $Q_{\rm O}$ is transformed to the expected output of the target state, and the state on $Q_{\rm C}$ remains the same as the input of the control state. Here, $U_{\rm F}$ is called a feedforward operation because it is determined by the measurement outcomes s_1 and s_2.

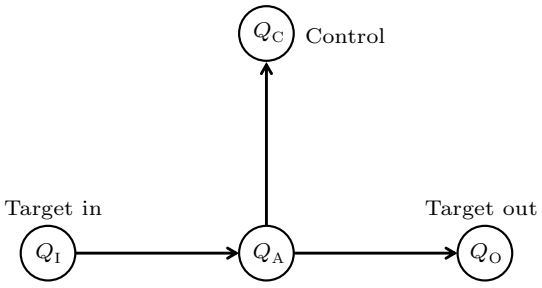


Fig. 1. The basic idea of the standard one-way CNOT gate. Qubits $Q_{\rm I}$ and $Q_{\rm O}$ serve as the input and output ports of the target state, respectively. $Q_{\rm C}$ serves as the control qubit, and $Q_{\rm A}$ is an ancilla qubit. The CZ gate is represented by the arrow starting from the control qubit and pointing to the target qubit.

In our previous work,[44] to realize this one-way CNOT gate on an on-cloud IBMQ superconducting quantum processor, which by that time did not support feedforward operations, we have replaced feedforward operations with delayed-measurement operations. The basic idea of delayed-measurement operation (see Fig. 2) is that a conditional single-qubit Hermitian operation controlled by the measurement result of another qubit can be replaced by a quantum controlled-gate between the two qubits before the measurement operation.

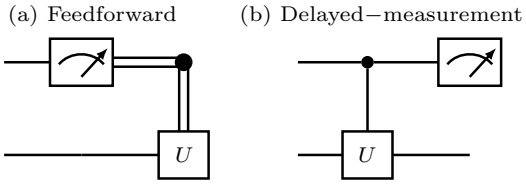


Fig. 2. Delayed-measurement method (b) compared to feedforward method (a).

We would like to emphasize an important advantage of the delayed-measurement operation over the corresponding feedforward operation, including its indirect realization via the post-selection method.[47–51] To carry out a feedforward operation, we need to measure a qubit, and the specific further operation is decided by the measurement result. Thus, the measurement error here would lead to an incorrect operation in the next step. However, for the delayed-measurement operation, the measurement operation acts only as a collapse operation on the possible superposition state on the measured

qubit, regardless of the readout. Thus, the measurement error would not affect the operations required after the measurement. Moreover, the delayed-measurement protocol avoids the limitation of many quantum processors, including the BAQIS Quafu processors, which yet cannot carry out quantum operations controlled by the classical register.

3. Modified one-way quantum computing with Bell state

Before introducing the modified one-way CNOT gate of one-way quantum computing, we first introduce the concept of the Bell gate, which will be useful in the following discussion. A Bell gate U_{jk}^{Bell} constructs different Bell states on the physical qubits Q_j and Q_k based on the initially input states:

$$\begin{cases} |0\rangle_j|0\rangle_k \to \frac{1}{\sqrt{2}}(|0\rangle_j|0\rangle_k + |1\rangle_j|1\rangle_k), \\ |0\rangle_j|1\rangle_k \to \frac{1}{\sqrt{2}}(|0\rangle_j|1\rangle_k + |1\rangle_j|0\rangle_k), \\ |1\rangle_j|0\rangle_k \to \frac{1}{\sqrt{2}}(|1\rangle_j|0\rangle_k - |0\rangle_j|1\rangle_k), \\ |1\rangle_j|1\rangle_k \to \frac{1}{\sqrt{2}}(|1\rangle_j|1\rangle_k - |0\rangle_j|0\rangle_k), \end{cases} \tag{3}$$

where $|0\rangle_j$, $|1\rangle_j$, $|0\rangle_k$, and $|1\rangle_k$ denote the initial input states of the physical qubit Q_j and Q_k. A Bell gate can be realized based on a quantum logic circuit, as shown in Fig. 3. We first apply a Z-flip gate and a Hadamard gate on qubits Q_j and Q_k, respectively, followed by a controlled-Z (CZ) gate between qubits Q_j and Q_k. Then, we apply another Hadamard gate on qubit Q_j, and again carry out a CZ gate on the two qubits. Finally, after applying a Hadamard gate on qubit Q_k, we achieve a Bell gate between qubits Q_j and Q_k.

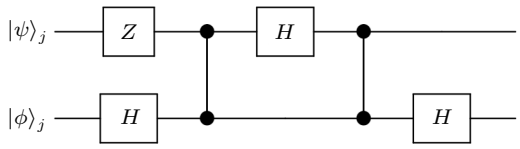


Fig. 3. Circuit model of the Bell gate with input states $|\psi\rangle_j$ and $|\phi\rangle_k$. Here, Z and H represent the Z-flip and Hadamard gates, respectively. Two solid circles connected by a solid line denote a two-qubit CZ gate.

Note that the theoretical proposal suggests that a Bell gate can be implemented by qubit-cavity systems in the ultrastrong coupling regime.[52] This signifies that although the Bell gate brings a quarter of the total circuit depth in the circuit model, the circuit depth may significantly decrease by applying a Bell gate in the qubit-cavity system.

Based on the Bell gate, reference [26] presents their protocol for the modified one-way CNOT gate. As described in Fig. 4, the modified one-way CNOT gate can be achieved by considering only three qubits Q_{I}, Q_{O}, and Q_{C}. The quantum circuit implementation of the modified CNOT gate is shown in Fig. 5. We first apply a Bell gate on qubits Q_{I} and Q_{O} with initial states $|i\rangle_{\text{I}}$ and $|0\rangle_{\text{O}}$. After the Bell gate, a CZ gate is applied on Q_{O} and Q_{C}. Note that the CZ gate here is defined as $U'_{\text{CZ}} = I\otimes|1\rangle\langle 1| + Z\otimes|0\rangle\langle 0|$, which is different from the conventional definition, as we have used in Section 2. This non-conventional CZ gate can be realized by applying X gates on both qubits before and after a conventional CZ gate, as shown in Fig. 5. Now, the quantum state of the 3-qubit system becomes

$$|\Psi\rangle = \frac{1}{\sqrt{2}}[|i_Z\rangle_{\text{I}}|0_Z\rangle_{\text{O}} + (-1)^i|(i\oplus 1)_Z\rangle_{\text{I}}|1_z\rangle_{\text{O}}]\,|j_Z\rangle_{\text{C}}, \tag{4}$$

where $|j_Z\rangle_{\text{C}}$ is an initial state of Q_{C}. Here, we denote the states with the subscript Z (X) to indicate that the states are represented using the $\sigma_{z(x)}$ basis.

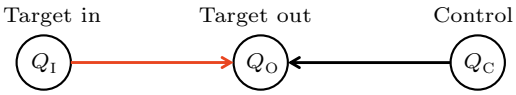


Fig. 4. The basic idea of the modified one-way CNOT gate. Qubit Q_{I} and Q_{O} play the role of the input and output of the target state, respectively, while qubit Q_{C} is the control qubit. The red arrow represents a Bell gate between qubits Q_{I} and Q_{O}, and the black arrow represents a non-conventional CZ gate between qubits Q_{C} and Q_{O}. Both arrows start at the control qubit and end at the target qubit.

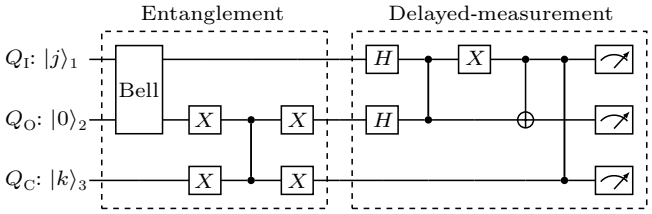


Fig. 5. Quantum logic circuit for implementing the modified one-way CNOT gate. We denote the three qubits from top to bottom as Q_1 to Q_3, respectively. Q_1 and Q_2 serve as the input and output of the target state, respectively, while Q_3 carries the control state.

Afterwards, we measure qubit Q_{I} under the σ_x basis, and the state becomes

$$\begin{aligned} |\Phi\rangle = \frac{1}{\sqrt{2}}\big[&(-1)^{j+1}|i_z\rangle_{\text{I}}|0_z\rangle_{\text{O}} \\ &+(-1)^i|(i\oplus 1)_z\rangle_{\text{I}}|1_z\rangle_{\text{O}}\big]\,|j_z\rangle_{\text{C}}. \end{aligned} \tag{5}$$

Then, we apply a Hadamard gate on qubit Q_{O}, transforming the state into

$$\begin{aligned} |\Phi'\rangle = \frac{(-1)^{i\cdot s}}{2}&|s_x\rangle_{\text{I}}\{[(-1)^{j+s+1}+(-1)^i]|0_z\rangle_{\text{O}} \\ &+[(-1)^{j+s+1}-(-1)^i]|1_z\rangle_{\text{O}}\}\,|j_z\rangle_{\text{C}}. \end{aligned} \tag{6}$$

Finally, when $s=0$, the corresponding feedforward operation, $U_{\text{F}}^{(s=0)} = -X_{\text{O}}Z_{\text{C}}$, acts on $|\Phi'\rangle$. Otherwise, we apply the feedforward operation $U_{\text{F}}^{(s=1)} = -Z_{\text{O}}$. After the feedforward operation, the outputs of the one-way CNOT gate on qubits Q_{O} and Q_{C} become

$$|\Phi\rangle_{\text{out}} = |s_x\rangle_{\text{I}}|(i\oplus j)_z\rangle_{\text{O}}\,|j_z\rangle_{\text{C}}. \tag{7}$$

As one can see, the effect of the above operations finally generates the output states satisfying the definition of the CNOT gate:

$$U_{\text{CNOT}} = I\otimes|0\rangle\langle 0| + Z\otimes|1\rangle\langle 1|, \tag{8}$$

and thus, we successfully realize a one-way CNOT gate.

Finally, we briefly explain why we call this approach a "modified" one-way CNOT gate. As mentioned before, one-way quantum computing is based on cluster states. A standard cluster state is defined by the eigenfunction[8]

$$K^{(a)}\,|\phi_\kappa\rangle_{\mathcal{C}} = (-1)^{\kappa_a}\,|\phi_\kappa\rangle_{\mathcal{C}}\,, \tag{9}$$

with the correlation operator

$$K^{(a)} = \sigma_x^{(a)} \otimes_{b\in\mathcal{G}_a} \sigma_z^{(b)}, \tag{10}$$

where $\mathcal{C}$ represents the cluster state, $\kappa := \{\kappa_a = 0, 1 | a \in \mathcal{C}\}$ is a set of binary parameters that specifies the cluster state, and $\mathcal{G}_a$ describes the neighboring qubits of qubit a. The entangled state utilized in the above protocol does not strictly obey the definition of the cluster state. For example, for $i = 0$, we find that

$$\begin{aligned} K^{(I)}\,|\Psi\rangle \;&=\; \frac{1}{\sqrt{2}}[|1_z\rangle_{\rm I}|0_z\rangle_{\rm O} - |0_z\rangle_{\rm I}|1_z\rangle_{\rm O}]\,|j_z\rangle_{\rm C} \\ &\neq\; (-1)^{\kappa_{\rm I}}\,|\Psi\rangle\,. \end{aligned} \tag{11}$$

However, since the CNOT gate can still be achieved by applying single-qubit measurements on the entangled state, without loss of generality, we can call the state and the protocol "modified".

4. Realization of the one-way CNOT gates with Quafu

Over the last decade, cloud-based quantum computers have been released by many academic organizations and commercial companies, e.g., D-Wave,[53] IBM,[54] Rigetti,[55] BAQIS,[56] and IonQ.[57] One can manipulate their devices by designing a quantum circuit with unitary-logic gates. Many quantum information tasks have been achieved using their devices, for example, quantum simulations,[58,59] fault-tolerant gates,[60] and quantum chemistry.[61]

As we have mentioned above, although the Quafu quantum computing platform provides a complete set of single-qubit and two-qubit quantum logic gates that form universal quantum gates, quantum operations controlled by classical bits (or classical register) are yet unavailable. In other words, neither standard nor modified one-way CNOT gate can be implemented by using the feedforward operation. Thus, similar to our previous work, we use the delayed-measurement approach to replace the feedforward operation.[44,62]

We introduce the delayed-measurement modified one-way CNOT gate using the 136-qubit Quafu processor called Baiwang. According to the status of Baiwang, we select three-in-a-row qubits to carry out our quantum logical circuit, numbered 114, 115, and 126, as shown in Fig. 6. These three qubits show the lowest average two-qubit gate error rates among Baiwang when we execute the circuit. At the beginning of the process, Q_{114}, Q_{115}, and Q_{126} serve as functional qubits $Q_{\rm O}$, $Q_{\rm I}$, and $Q_{\rm C}$, respectively, so we initialize these qubits to the corresponding initial states.

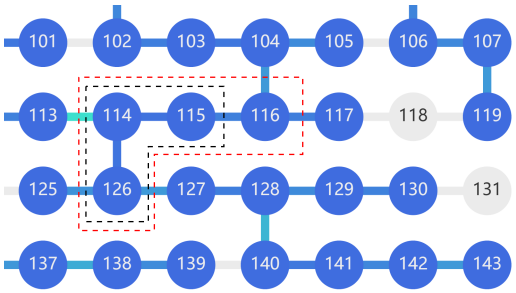


Fig. 6. Topological structure of the right-down corner of the 136-qubit on-cloud superconducting processor Quafu Baiwang. The complete structure can be found on the Quafu website.[46] The black (red) dash box marks out the physical qubits utilized to build the modified (standard) one-way CNOT gate.

The quantum circuit implementation of a delayed-measurement modified one-way CNOT gate is schematically shown in Fig. 7. After the system is entangled to the modified cluster state following the steps in Section 3, we apply Hadamard gates to qubits Q_{115} and Q_{114}. Note that the purpose of inserting Hadamard gates is different for the individual qubits Q_{115} and Q_{114}. For Q_{115}, the goal is to rotate the measurement basis to the X-axis. For Q_{114}, inserting a Hadamard gate is the original requirement in the modified one-way CNOT gate [see Eq. (6)].

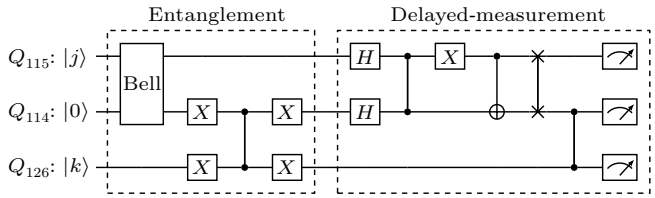


Fig. 7. Quantum logic circuit for implementing the modified one-way CNOT gate on the Quafu superconducting processor Baiwang. Compared to Fig. 5, due to the limited connectivity of Baiwang, here we insert a SWAP gate between physical qubits Q_{115} and Q_{114} after applying the delayed-measurement operation between $Q_{\rm I}$ and $Q_{\rm O}$ acted by Q_{115} and Q_{114}, respectively. Thus, we effectively carry out the feedforward between $Q_{\rm I}$ and $Q_{\rm C}$, which was originally acted by non-neighboring physical qubits Q_{115} and Q_{126}, respectively.

The first delayed-measurement operation can be realized by applying a non-conventional CZ gate, as mentioned in Section 3, between qubits Q_{115} and Q_{114}. This operation corresponds to the feedforward $Z_{\rm O}$ under the condition $s = 1$. The second delayed-measurement operation, which can be written as the feedforward $X_{\rm O}$ under the condition $s = 0$, can be decomposed by a X gate on qubit Q_{115}, followed by a CNOT gate between qubits Q_{115} and Q_{114}.

Note that due to the non-fully connected structure of the Quafu Baiwang, we need to apply a SWAP gate between

qubits Q_{115} and Q_{114}. Thus, we can perform a CZ gate between qubits $Q_{\rm I}$ and $Q_{\rm C}$, which now correspond to physical qubits Q_{114} and Q_{126} in Baiwang. This corresponds to the final step of the feedforward operation: $Z_{\rm C}$ under condition $s=0$. By measuring qubit Q_{114}, which serves as the input qubit $Q_{\rm I}$, the three-qubit system collapses to the state with respect to its corresponding measurement outcomes.

Here, we note that we did not consider the negative signs of the required feedforward operations, since both negative signs simply import an overall π phase to the final state. This does not affect the result of the gate.

For comparison, we also perform the delayed-measurement standard one-way CNOT gate using Quafu Baiwang. Here, we select physical qubits Q_{114}, Q_{115}, Q_{116}, and Q_{126} to perform the gate, as marked in Fig. 6. The quantum circuit to realize a delayed-measurement standard one-way CNOT gate is shown in Fig. 8. At the beginning of the process, the four physical qubits serve as $Q_{\rm A}$, $Q_{\rm I}$, $Q_{\rm C}$, and $Q_{\rm O}$, respectively. After initializing the qubits, we first perform CZ gates between Q_{114}–Q_{115} and Q_{114}–Q_{126}. Then, we carry out a SWAP gate between Q_{114} and Q_{115}, followed by another CZ gate between Q_{115} and Q_{116}, a.k.a. $Q_{\rm A}$ and $Q_{\rm C}$, and complete the entanglement process.

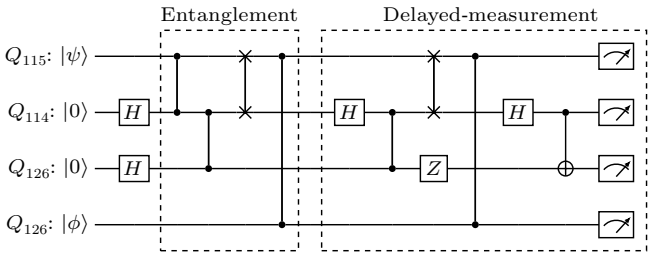


Fig. 8. Quantum logic circuit for implementing the standard one-way CNOT gate on the Quafu superconducting processor Baiwang. Initially, physical qubits Q_{115}, Q_{114}, Q_{126} and Q_{116} act as logical qubits $Q_{\rm I}$, $Q_{\rm A}$, $Q_{\rm O}$ and $Q_{\rm C}$, respectively. Here, we insert a SWAP gate between physical qubits Q_{115} and Q_{114} after entangling Q_{115}, Q_{114} and Q_{126} in order to carry out further operation between $Q_{\rm A}$–$Q_{\rm C}$ and $Q_{\rm I}$–$Q_{\rm O}$. After applying the delayed-measurement operation between $Q_{\rm I}$ and $Q_{\rm O}$ acted by Q_{115} and Q_{114}, respectively, the characters of Q_{115} and Q_{114} are swapped back, so that the delayed-measurement operations between $Q_{\rm I}$–$Q_{\rm C}$ and $Q_{\rm A}$–$Q_{\rm O}$ become available.

Then, we apply a Hadamard gate to Q_{114}, followed by a CZ gate between Q_{114} and Q_{126}, and a Z gate on Q_{126}. Next, we swap Q_{114} and Q_{115} again and perform a CZ gate between Q_{115} and Q_{116}. In this way, we equivalently performed the feedforward operations related to $Q_{\rm I}$: $Z_{\rm O}^{s_1+1}\otimes Z_{\rm C}^{s_1}$. Next, by applying a Hadamard gate on Q_{114} and a CNOT gate between Q_{114} and Q_{126}, we equivalently realize the rest of the feedforward, $X_{\rm O}^{s_2}$. Finally, by measuring the qubits, we complete the process of the delayed-measurement standard one-way CNOT gate, and obtain the final output of the target state and the control state on qubits Q_{126} and Q_{116}, respectively.

Figure 9 presents the results of the standard and modified delayed-measurement one-way CNOT gates obtained from Quafu Baiwang, and the detailed data are shown in Table 1. We have performed both gates with different inputs: $|00\rangle$, $|01\rangle$, $|10\rangle$, and $|11\rangle$. Here, an input $|ij\rangle$ represents that the input of the target state is $|i\rangle$, and the input of the control state is $|j\rangle$. According to Fig. 9 and Table 1, the modified one-way CNOT gate shows a clear advantage over its standard counterpart.

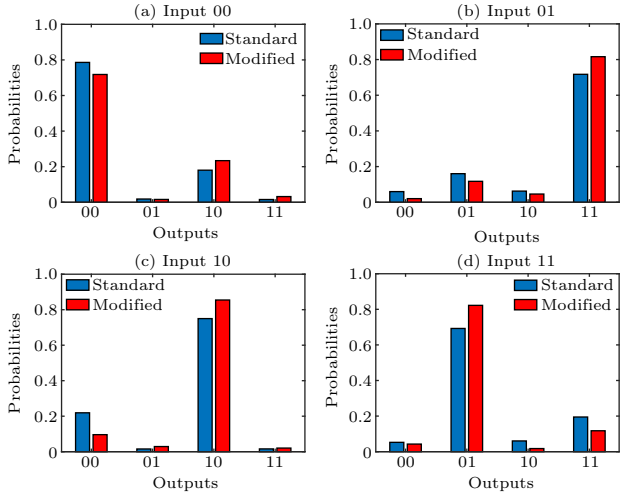


Fig. 9. Result obtained from Baiwang. The inputs of qubit $Q_{\rm I}$ and qubit $Q_{\rm C}$ are (a) $|00\rangle$, (b) $|01\rangle$, (c) $|10\rangle$, and (d) $|11\rangle$, respectively. The red bars correspond to the results of the modified one-way CNOT gates, while the blue bars correspond to their standard counterparts. The output jk represents the readouts of qubits $Q_{\rm O}$ ($|j\rangle$) and $Q_{\rm C}$ ($|k\rangle$).

Table 1. Probability distributions for the standard and modified one-way CNOT gates implemented on Baiwang. Here, "Input $|ij\rangle$" represents that the input of the target state and the control state are $|i\rangle$ and $|j\rangle$, respectively. The $|kl\rangle$ in the second to fifth columns denote the measurement results kl.

Input $\|00\rangle$	$\|00\rangle$	$\|01\rangle$	$\|10\rangle$	$\|11\rangle$
Standard	0.7860	0.0182	0.1803	0.0155
Modified	0.7182	0.0159	0.2339	0.0320
Input $\|01\rangle$	$\|00\rangle$	$\|01\rangle$	$\|10\rangle$	$\|11\rangle$
Standard	0.0598	0.1603	0.0626	0.7173
Modified	0.0204	0.1174	0.0461	0.8161
Input $\|10\rangle$	$\|00\rangle$	$\|01\rangle$	$\|10\rangle$	$\|11\rangle$
Standard	0.2191	0.0153	0.7499	0.0157
Modified	0.0960	0.0290	0.8546	0.0204
Input $\|11\rangle$	$\|00\rangle$	$\|01\rangle$	$\|10\rangle$	$\|11\rangle$
Standard	0.0524	0.6925	0.0603	0.1948
Modified	0.0427	0.8223	0.0175	0.1175

5. Advantage of modified one-way CNOT gate in large-scale one-way quantum computing

In order to study the advantage of the modified one-way CNOT gate over the standard one-way CNOT gate, we repeatedly carry out two one-way CNOT gates under individual noise channels: qubit decoherence, qubit measurement error, and depolarization error of the logic gates with the simulator. Here, both the one-way CNOT gates are delayed-measurement one-way CNOT gates.

First, we only consider the impact of qubit decoherence without taking into account the other noisy channels in the simulator. Under this condition, the coherence times T_1 and T_2 of all the qubits are set as 100 μs.

We separately carry out the standard one-way CNOT gates and the modified one-way CNOT gates. The initial input states of the target and control qubits are $|0\rangle$ and $|1\rangle$, respectively; thus, the expected output of the control state remains $|1\rangle$. On the other hand, the expected output of the target state, after performing an odd (even) number of CNOT gates, is $|1\rangle$ (odd) or $|0\rangle$ (even). The results of our simulations are shown in Fig. 10(a), in which the curves indicate the evolution of the probability of obtaining the expected results increasing the amounts of repetition of the one-way CNOT gates. From our numerical results, one can see that the modified one-way CNOT gate is more robust against qubit decoherence than the standard one-way CNOT gate.

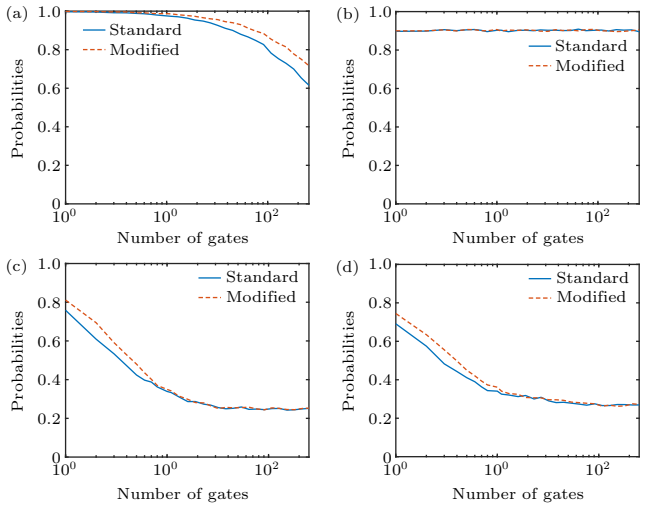


Fig. 10. Numerical results of the processes carrying out the delayed-measurement standard and modified one-way CNOT gates repeatedly, with the existence of (a) qubit decoherence, where the coherence times T_1 and T_2 are both set as 100 μs; (b) qubit measurement error, where the measurement error is set as 5%; (c) depolarization error of the logic gates, where the error rates of the 1-qubit gate sand 2-qubit gates are set as 1% and 10%, respectively; (d) all the noises above. The blue (red) line represents the probability of the expected output after performing the standard (modified) delayed-measurement one-way CNOT gate for the number of times repeating the gate. No other type of error is taken into account here.

Second, we only consider the impact of qubit measurement error in one-way CNOT gates. The error rate of a single-qubit measurement is considered to be 5%. We have pointed out in Section 2 that during a delayed-measurement one-way computing process, most of the measurement operations simply serve as collapse operations, and the results are no longer mentioned in the following process. Thus, the measurement error of these operations does not affect the final result. The only measurement errors that affect the final result are the measurements reading the results at the end of the entire process. Thus, the effects of the measurement error on both processes are expected to be similar, no matter how many times we repeat the one-way CNOT gate.

Here, we present the numerical simulation results to support the above statement. As shown in Fig. 10(b), the measurement error is independent of the repeated delay-choice one-way CNOT gates, which supports our statement. This numerically implies an important advantage of the delayed-measurement method in one-way quantum computing.

Third, we consider the depolarization error of the logic gates. The error rates for the 1-qubit gate and 2-qubit gate are 1% and 10%, respectively. The numerical results shown in Fig. 10(c) indicate that compared to its standard counterpart, the modified one-way CNOT gate behaves more robustly against the depolarization error of the logic gates.

Finally, we put the above noises together and numerically simulated the process again. The results are shown in Fig. 10(d). Once again, these clearly show the advantage of the modified one-way CNOT gate over its standard counterpart.

These numerical results indicate that the modified one-way CNOT gate, in general, outperforms the standard CNOT gate in large-scale one-way quantum computing and has clear potential for improving the fidelity of the large-scale one-way quantum computing processes in the noisy intermediate-scale quantum (NISQ) era.[63,64]

6. Conclusion

Using the programmable Quafu processor Baiwang, we have demonstrated the operation of a modified one-way CNOT gate with the delayed-measurement method. Since the number of qubits participating in the modified cluster states is less than the number of the standard one, the complexity of the circuit model (i.e., circuit depth) decreases. In addition, the number of SWAP operations also declines for the construction of the cluster state. Our results obtained from Baiwang not only show that the modified one-way CNOT gate can be efficiently demonstrated on the Quafu processor but also prove the advantage of the modified protocol against the standard one. We have also numerically demonstrated the advantage of the modified one-way CNOT gate in large-scale one-way quantum computing, as well as the advantage of the delayed-measurement method over the feedforward method in the robustness against measurement errors.

Acknowledgments

The authors appreciate Franco Nori for the valuable discussions. Project supported by the National Natural Science Foundation of China (Grant Nos. 92265207 and T2121001) and Beijing Natural Science Foundation (Grant No. Z200009).

References

[1] Vandersypen L M K and Chuang I L 2005 *Rev. Mod. Phys.* **76** 1037
[2] Saffman M, Walker T G and Mølmer K 2010 *Rev. Mod. Phys.* **82** 2313

[3] Reiserer A and Rempe G 2015 *Rev. Mod. Phys.* **87** 1379
[4] Blais A, Grimsmo A L, Girvin S M and Wallraff A 2021 *Rev. Mod. Phys.* **93** 025005
[5] Li Y, Xin T, Qiu C, Li K, Gangqin L, Li J, Wan Y and Lu D 2023 *Fundamental Res.* **3** 229
[6] Raussendorf R and Briegel H J 2001 *Phys. Rev. Lett.* **86** 5188
[7] Briegel H J and Raussendorf R 2001 *Phys. Rev. Lett.* **86** 910
[8] Raussendorf R, Browne D E and Briegel H J 2003 *Phys. Rev. A* **68** 022312
[9] Newman M, de Castro L A and Brown K R 2020 *Quantum* **4** 295
[10] Bourassa J E, Alexander R N, Vasmer M, Patil A, Tzitrin I, Matsuura T, Su D, Baragiola B Q, Guha S, Dauphinais G, Sabapathy K K, Menicucci N C and Dhand I 2021 *Quantum* **5** 392
[11] Zwerger M, Briegel H J and Dür W 2013 *Phys. Rev. Lett.* **110** 260503
[12] Ferguson R R, Dellantonio L, Balushi A A, Jansen K, Dür W and Muschik C A 2021 *Phys. Rev. Lett.* **126** 220501
[13] Asavanant W, Shiozawa Y, Yokoyama S, Charoensombutamon B, Emura H, Alexander R N, Takeda S, Yoshikawa J I, Menicucci N C, Yonezawa H and Furusawa A 2019 *Science* **366** 373
[14] Larsen M V, Guo X, Breum C R, Neergaard-Nielsen J S and Andersen U L 2019 *Science* **366** 369
[15] Zhou Z Y, Gneiting C, You J Q and Nori F 2023 *Phys. Rev. A* **108** 023704
[16] Walther P, Resch K J, Rudolph T, Schenck E, Weinfurter H, Vedral V, Aspelmeyer M and Zeilinger A 2005 *Nature* **434** 169
[17] Prevedel R, Walther P, Tiefenbacher F, Böhi P, Kaltenbaek R, Jennewein T and Zeilinger A 2007 *Nature* **445** 65
[18] Tame M S, Prevedel R, Paternostro M, Böhi P, Kim M S and Zeilinger A 2007 *Phys. Rev. Lett.* **98** 140501
[19] Chen K, Li C M, Zhang Q, Chen Y A, Goebel A, Chen S, Mair A and Pan J W 2007 *Phys. Rev. Lett.* **99** 120503
[20] Vallone G, Pomarico E, De Martini F and Mataloni P 2008 *Phys. Rev. Lett.* **100** 160502
[21] Kaltenbaek R, Lavoie J, Zeng B, D B S and Resch K J 2010 *Nat. Phys.* **6** 850
[22] Tame M S, Bell B A, Di Franco C, Wadsworth W J and Rarity J G 2014 *Phys. Rev. Lett.* **113** 200501
[23] Lanyon B P, Jurcevic P, Zwerger M, Hempel C, Martinez E A, Dür W, Briegel H J, Blatt R and Roos C F 2013 *Phys. Rev. Lett.* **111** 210501
[24] Ju C, Zhu J, Peng X, Chong B, Zhou X and Du J 2010 *Phys. Rev. A* **81** 012322
[25] Wei T C 2021 *Measurement-based quantum computation* (Oxford University Press)
[26] Albarrán-Arriagada F, Alvarado Barrios G, Sanz M, Romero G, Lamata L, Retamal J C and Solano E 2018 *Phys. Rev. A* **97** 032320
[27] You J and Nori F 2011 *Nature* **474** 589
[28] Devoret M H, Wallraff A and Martinis J M 2004 arXiv:cond-mat/0411174 [cond-mat.mes-hall]
[29] Buluta I, Ashhab S and Nori F 2011 *Rep. Prog. Phys.* **74** 104401
[30] Gu X, Kockum A F, Miranowicz A, Liu Y X and Nori F 2017 *Phys. Rep.* **718-719** 1
[31] Kockum A F and Nori F 2019 *Fundamentals and Frontiers of the Josephson Effect* edn. Tafuri (Springer) pp. 703–741
[32] Tanamoto T, Liu Y X, Fujita S, Hu X and Nori F 2006 *Phys. Rev. Lett.* **97** 230501
[33] You J Q, Wang X B, Tanamoto T and Nori F 2007 *Phys. Rev. A* **75** 052319
[34] Tanamoto T, Liu Y X, Hu X and Nori F 2009 *Phys. Rev. Lett.* **102** 100501
[35] Zhang X L, Gao K L and Feng M 2006 *Phys. Rev. A* **74** 024303
[36] Chen G, Chen Z, Yu L and Liang J 2007 *Phys. Rev. A* **76** 024301
[37] Li Z, Ma S L, Yang Z P, Fang A P, Li P B, Gao S Y and Li F L 2016 *Phys. Rev. A* **93** 042305
[38] Lähteenmäki P, Paraoanu G S, Hassel J and Hakonen P J 2016 *Nature Communications* **7** 12548
[39] Yang Z P, Li Z, Ma S L and Li F L 2017 *Phys. Rev. A* **96** 012327
[40] Wang Y, Li Y, Yin Z Q and Zeng B 2018 *npj Quantum Information* **4** 46
[41] Gong M, Chen M C, Zheng Y, Wang S, Zha C, Deng H, Yan Z, Rong H, Wu Y, Li S, Chen F, Zhao Y, Liang F, Lin J, Xu Y, Guo C, Sun L, Castellano A D, Wang H, Peng C, Lu C Y, Zhu X and Pan J W 2019 *Phys. Rev. Lett.* **122** 110501
[42] Besse J C, Reuer K, Collodo M C, Wulff A, Wernli L, Copetudo A, Malz D, Magnard P, Akin A, Gabureac M, Norris G J, Cirac J I, Wallraff A and Eichler C 2020 *Nat. Commun.* **11** 4877
[43] Shirai S, Zhou Y, Sakata K, Mukai H and Tsai J S 2021 arXiv:2105.08609 [quant-ph]
[44] Yang Z P, Ku H Y, Baishya A, Zhang Y R, Kockum A F, Chen Y N, Li F L, Tsai J S and Nori F 2022 *Phys. Rev. A* **105** 042610
[45] Li Y, Wang Z, Bao Z, Wu Y, Wang J, Yang J, Xiong H, Song Y, Zhang H and Duan L 2023 *Chip* **2** 100063
[46] Quafu
[47] Zhao Y Y, Ku H Y, Chen S L, Chen H B, Nori F, Xiang G Y, Li C F, Guo G C and Chen Y N 2020 *npj Quantum Inf.* **6** 77
[48] Ku H Y, Weng H C, Shih Y A, Kuo P C, Lambert N, Nori F, Chuu C S and Chen Y N 2021 *Phys. Rev. Res.* **3** 043083
[49] Ku H Y, Hsieh C Y, Chen S L, Chen Y N and Budroni C 2022 *Nat. Commun.* **13** 4973
[50] Ku H Y, Hsieh C Y and Budroni C 2023 arXiv:2308.02252 [quant-ph]
[51] Hsieh C Y, Ku H Y and Budroni C 2023 arXiv:2309.06191 [quant-ph]
[52] Albarrán-Arriagada F, Lamata L, Solano E, Romero G and Retamal J C 2018 *Phys. Rev. A* **97** 022306
[53] King A D, Raymond J, Lanting T, Harris R, Zucca A, Altomare F, Berkley A J, Boothby K, Ejtemaee S, Enderud C, Hoskinson E, Huang S, Ladizinsky E, MacDonald A J R, Marsden G, Molavi R, Oh T, Poulin-Lamarre G, Reis M, Rich C, Sato Y, Tsai N, Volkmann M, Whittaker J D, Yao J, Sandvik A W and Amin M H 2023 *Nature* **617** 61
[54] Kandala A, Temme K, Córcoles A D, Mezzacapo A M C J and Gambetta J M 2019 *Nature* **567** 491
[55] Gold A, Paquette J P, Stockklauser A, Reagor M J, Alam M S, Bestwick A, Didier N, Nersisyan A, Oruc F, Razavi A, Scharmann B, Sete E A, Sur B, Venturelli D, Winkleblack C J, Wudarski F, Harburn M and Rigetti C 2021 *NPJ Quantum Information* **7** 142
[56] Chen C T, Shi Y H, Xiang Z, Wang Z A, Li T M, Sun H Y, He T S, Song X, Zhao S, Zheng D, Xu K and Fan H 2022 *Sci. China Phys. Mech. Astron.* **65** 110362
[57] Johri S, Debnath S, Mocherla A, SINGK A, Prakash A, Kim J and Kerenidis I 2021 *NPJ Quantum Information* **7** 122
[58] Ku H Y, Lambert N, Chan F J, Emary C, Chen Y N and Nori F 2020 *npj Quantum Information* **6** 98
[59] Meitei O R, Gard B T, Barron G S, Pappas D P, Economou S E, Barnes E and Mayhall N J 2021 *npj Quantum Information* **7** 155
[60] Harper R and Flammia S T 2019 *Phys. Rev. Lett.* **122** 080504
[61] Robert A, Barkoutsos P K, Woerner S and Tavernelli I 2021 *npj Quantum Information* **7** 38
[62] Chandarana P D, Baiju A A, Mukherjee S, Das A, Hegade N N and Panigrahi P K 2020 arXiv:2004.04625 [quant-ph]
[63] Xu K and Fan H 2022 *Chin. Phys. B* **31** 100304
[64] Law J W Z, Kim K H, Shrotriya H and Kwek L C 2022 *AAPPS Bull.* **32** 27